Sosioedukasi
JURNAL ILMIAH ILMU PENDIDIKAN DAN SOSIAL
ISSN: 2086-6135 E-ISSN: 2541-612x
Volume 15 No. 1. Maret 2026 https://ejournal.unibabwi.ac.id/index.php/sosioedukasi/index

GEOAI-BASED SPATIOTEMPORAL ASSESSMENT OF SURFACE URBAN HEAT ISLAND DYNAMICS AND LAND COVER CHANGE USING GOOGLE EARTH ENGINE: EVIDENCE FROM MANADO CITY, INDONESIA

Fidelia Anninda Fabiolani[a*], Winsy Weku[b], Eric Alfonsius[c]

[a,b,c] Department of Information Systems, Faculty of Mathematics and Natural Sciences, Sam Ratulangi University, Indonesia

[*a]*E-mail:* fideliafabiolani106@student.unsrat.ac.id
(*) Corresponding Author
fideliafabiolani106@student.unsrat.ac.id

ARTICLE HISTORY
Received : 23-07-2026
Revised : 23-08-2026
Accepted : 30-08-2026

KEYWORDS
SUHI, LST, Google Earth Engine, Random Forest, Land Cover Change, Urban Climate, Tropical Coastal City.

ABSTRACT
Rapid urbanization has significantly transformed land cover patterns and intensified the Surface Urban Heat Island (SUHI) phenomenon in many tropical cities, posing increasing environmental and public health challenges. However, comprehensive long-term assessments integrating land cover dynamics, land surface temperature (LST), and SUHI using cloud-based geospatial platforms remain limited, particularly in rapidly developing cities of eastern Indonesia. This study investigates the spatiotemporal relationship between land cover change and SUHI dynamics in Manado City, Indonesia, between 2000 and 2023 by integrating Landsat imagery, Google Earth Engine (GEE), and a GeoAI-based Random Forest classification approach. Landsat 7 ETM+ and Landsat 9 OLI/TIRS datasets were processed to generate land cover maps and retrieve LST, while SUHI intensity was derived from spatial thermal anomalies. Classification accuracy was evaluated using confusion matrices, achieving Overall Accuracy of 95.28% (Kappa = 0.915) for 2000 and 92.00% (Kappa = 0.870) for 2023. Results reveal a substantial decline in vegetation from 10.844,523 ha (75,69%) to 9.724,045 ha (67,87%), accompanied by an expansion of built-up land from 3.374,629 ha (23,55%) to 3.939,957 ha (27,49%). These land cover transformations corresponded with an increase in average LST from 33.79°C to 37.08°C and a spatial expansion of high-intensity SUHI zones from the urban core toward developing suburban districts. Subdistrict-level analysis further shows considerable spatial heterogeneity in thermal conditions, with the greatest warming occurring in the most intensively developed areas. The results confirm that urban expansion and vegetation loss are the principal drivers of increasing SUHI intensity in Manado, supporting climate-responsive urban planning and sustainable land-use management

Sosioedukasi
JURNAL ILMIAH ILMU PENDIDIKAN DAN SOSIAL
ISSN: 2086-6135 E-ISSN: 2541-612x
Volume 15 No. 1. Maret 2026 https://ejournal.unibabwi.ac.id/index.php/sosioedukasi/index

INTRODUCTION

Rapid urbanization has become one of the most significant drivers of environmental transformation worldwide, resulting in profound changes in lsand cover and urban thermal conditions. The conversion of vegetated landscapes into impervious built-up surfaces alters the surface energy balance by reducing evapotranspiration, increasing heat storage, and modifying radiative properties, ultimately intensifying the Surface Urban Heat Island (SUHI) phenomenon (Stewart & Mills, 2021). SUHI is characterized by elevated land surface temperatures (LST) in urban areas relative to their surrounding rural environments and has become a critical environmental issue because of its implications for energy consumption, ecosystem degradation, climate resilience, and human health (Wardhana et al., 2021). As global temperatures continue to rise due to climate change, understanding the spatial dynamics of SUHI has become increasingly important for sustainable urban planning and environmental management.

Remote sensing technology has become the primary approach for investigating SUHI because it enables long-term, large-scale, and spatially explicit observations of land surface temperature and land cover dynamics (Darmawan et al., 2024). Landsat satellite imagery, in particular, provides a consistent historical archive that facilitates multi-temporal analyses of urban environmental change. More recently, cloud-based geospatial platforms such as Google Earth Engine (GEE) have significantly improved the efficiency of processing large satellite datasets by integrating data storage, image preprocessing, spatial analysis, and visualization within a single computational environment. Simultaneously, advances in Geospatial Artificial Intelligence (GeoAI), especially machine learning algorithms such as Random Forest, have substantially enhanced land cover classification accuracy and enabled more reliable monitoring of urban landscape transformations (Kartika et al., 2024).

Despite these advances, several important research gaps remain. First, many previous studies have focused primarily on either land cover classification or land surface temperature analysis independently, with relatively few integrating both datasets into a comprehensive assessment of SUHI evolution over extended time periods. Second, although Google Earth Engine has become increasingly popular for urban thermal studies, the integration of GEE with GeoAI-based machine learning for simultaneous analysis of land cover dynamics and SUHI remains limited, particularly in medium-sized tropical cities. Third, existing SUHI studies in Indonesia have been concentrated mainly in western and central regions, whereas rapidly developing cities in eastern Indonesia have received comparatively little scientific attention despite experiencing accelerated urban growth and environmental transformation. Consequently, the spatial relationship between urban expansion, vegetation loss, and thermal variability in these cities remains insufficiently understood.

Manado City, the capital of North Sulawesi Province, provides an ideal case for addressing these research gaps. During the past two decades, rapid population growth and urban expansion (Badan Pusat Statistika, 2023) have transformed substantial portions of vegetated land into built-up areas, potentially intensifying urban thermal conditions. As a tropical coastal city with complex topography and heterogeneous urban development, Manado exhibits unique environmental characteristics that may influence the spatial distribution of SUHI differently from inland metropolitan areas. However, comprehensive studies integrating land cover change, land surface temperature, and SUHI dynamics using cloud-based GeoAI approaches remain unavailable for this region (Zhao et al., 2025).

Therefore, this study aims to analyze land cover change, Land Surface Temperature, and Surface Urban Heat Island dynamics in Manado City between 2000 and 2023 using Landsat imagery, Google Earth Engine, and a GeoAI-based Random Forest classifier. The findings are expected to improve understanding of the relationship between urban expansion and thermal conditions while providing scientific evidence to support sustainable urban planning and climate adaptation.

Sosioedukasi
JURNAL ILMIAH ILMU PENDIDIKAN DAN SOSIAL
ISSN: 2086-6135 E-ISSN: 2541-612x
Volume 15 No. 1. Maret 2026 https://ejournal.unibabwi.ac.id/index.php/sosioedukasi/index

METHOD

North Sulawesi Province is located between 1°30'–1°40' North Latitude and 124°40'–126°50' East Longitude. Based on its geographical position, the city of Manado is bordered by: to the north North Minahasa Regency; to the east North Minahasa Regency and Minahasa Regency; to the south Minahasa Regency; and to the west the Sulawesi Sea.

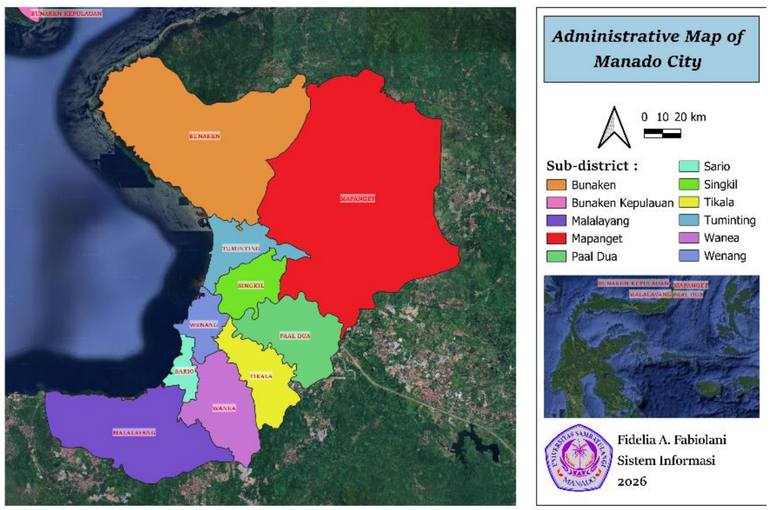

Figure 1 Administrative Map of Manado City

This study employed Landsat 7 ETM+ Collection 2 Level 2 imagery from 2000 and Landsat 9 OLI/TIRS Collection 2 Level 2 imagery from 2023, obtained from the United States Geological Survey (USGS, 2020) through Google Earth Engine (GEE). These datasets were used to analyze land cover, Land Surface Temperature (LST), and Surface Urban Heat Island (SUHI). The administrative boundary of Manado City, provided by the Geospatial Information Agency, was used to delineate the study area.

Image processing and spatial analysis were conducted using Google Earth Engine and QGIS. Google Earth Engine was used for image preprocessing, land cover classification, LST calculation, and SUHI analysis, while QGIS was used for spatial visualization and map layout preparation.

This study adopted a quantitative remote sensing approach to analyze changes in land cover, LST, and SUHI in Manado City between 2000 and 2023. Land cover was classified using the Random Forest algorithm into three classes: vegetation, built-up areas, and water (Safitri et al., 2022). Training samples were selected through purposive sampling (Rahman et al., 2022) based on visual interpretation of high-resolution Google Earth imagery, while NDVI, NDBI, and MNDWI were incorporated to improve class separability (Elwantyo et al., 2020). A total of 212 training and 106 testing samples were used for the 2000 classification, whereas 250 training and 125 testing samples were used for the 2023 classification. Classification accuracy was assessed using Overall Accuracy (OA), User's Accuracy (UA), and the Kappa coefficient based on the confusion matrix (Natun & Sumarlin, 2025).

Land Surface Temperature (LST) was calculated from the Landsat surface temperature band using Equation (1).

$$LST = \left(ST_{B_X} \times 0.00341802 + 149.0\right) - 273.15 \quad \text{.........(1)}$$

$$LST = \left(ST_{B_X} \times 0.00341802 + 149.0\right) - 273.15$$

Surface Urban Heat Island (SUHI) values were obtained by subtracting the mean LST of the study area from the LST of each pixel (Fawzi, 2017) using Equations (2)

$$\overline{LST} = \frac{\sum_{i=1}^{n} LST}{n} \tag{2}$$

Notes:
LST : Average surface temperature of the study area
$LSTi$: Surface temperature at the i-th pixel
n : Total number of pixels in the study area
and (3)

$$SUHI = LST_i - \overline{\mathrm{LST}} \tag{3}$$

Notes:
SUHI : SUHI Value
LST_i : Surface temperature value at pixel i
$\overline{\mathrm{LST}}$: Average surface temperature value of the study area

Subsequently, SUHI intensity was classified using the mean ± standard deviation method (Equations (4) and (5) into three categories: Non-SUHI, Potential SUHI, and SUHI. This method is considered stable and robust in classifying SUHI compared to other method (Lu et al., 2021).

$$\text{Upper Limit} = S\bar{U}HI + \sigma \tag{4}$$
$$\text{Lower Limit} = S\bar{U}HI - \sigma \tag{5}$$

Notes:
SUHI : Average SUHI value
σ : SUHI standard deviation

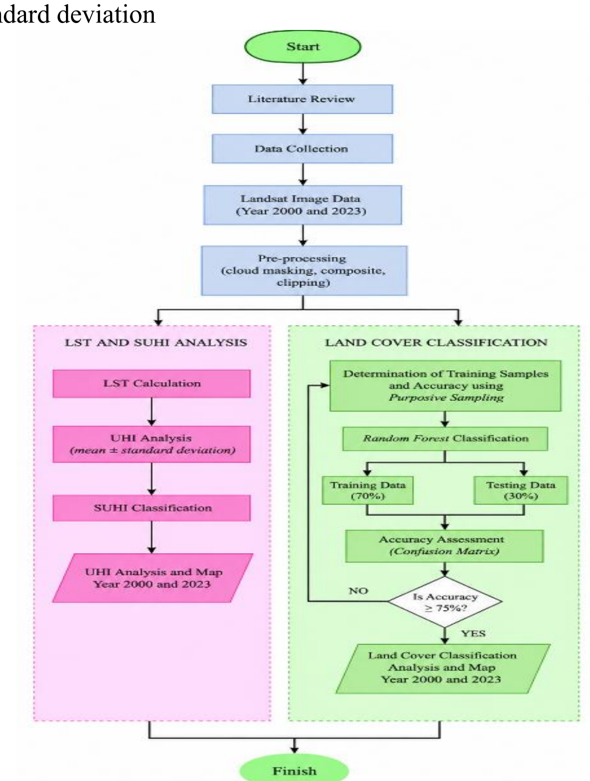

Figure 2 Research Flowchart

RESULTS AND DISCUSSION

Land Cover Classification

The results of the analysis of the land cover classification map, which is divided into three classes water, vegetation, and built-up land are shown in Table 3. The land cover classification results for 2000 indicate that vegetation was the dominant land cover type in Manado City, occupying 10.844,523 ha (75.69%) of the total study area. This extensive vegetation cover suggests that, at the beginning of the study period, much of the city still consisted of forests, agricultural land, and other green spaces that played an important role in regulating the local microclimate through evapotranspiration and shading. In contrast, built-up land covered 3.374,629 ha (23.55%), reflecting a relatively moderate level of urban development concentrated mainly within the city center and established residential areas. Water bodies represented only 108,051 ha (0.75%), indicating that aquatic features occupied only a small proportion of the administrative area. Overall, the 2000 land cover distribution characterizes Manado as a city where natural vegetation remained the predominant landscape, providing favorable environmental conditions and limiting excessive surface heating.

Table 1. Land Cover Analysis

Land Suitability Analysis 2000			
No.	Class	Area (ha)	%
1.	Water	108,051	0.75
2.	Vegetation	10.844,523	75.69
3.	Built-Up Land	3.374,629	23.55
Total		14.327,205	100
Land Suitability Analysis 2023			
No	Class	Area (ha)	%
1.	Water	663,2023	4.62
2.	Vegetation	9.724,0455	67.87
3.	Built-Up Land	3.939,9571	27.49
Total		14327.2050	100

Table source: Analysis Results, 2026

By 2023, the land cover composition had changed considerably, reflecting the impact of rapid urbanization during the 23-year study period. Although vegetation remained the largest land cover class, its extent declined to 9.724,0455 ha (67.87%), indicating a substantial reduction in green areas. Conversely, built-up land expanded to 3.939,9571 ha (27.49%), demonstrating continued urban expansion driven by population growth and infrastructure development. The most notable proportional increase occurred in water bodies, which expanded to 666.63 ha (4.62%). This increase may be associated with improved detection capabilities of Landsat 9 imagery, differences in tidal or seasonal water conditions, or the inclusion of additional coastal and inland water features during image classification. Despite vegetation remaining dominant, the increased proportion of impervious surfaces indicates an increasingly urbanized landscape with greater potential for elevated land surface temperatures and Surface Urban Heat Island (SUHI) formation.

Model Performance Evaluation

The confusion matrix indicates that the Random Forest classifier achieved high classification accuracy for both 2000 and 2023 (Table 2). In 2000, the classification reached an Overall Accuracy (OA) of 95.28% with a Kappa coefficient of 0.915, indicating almost perfect agreement between the classified map and the reference data. Water was classified perfectly, while vegetation and built-up land also showed high accuracy with only minor misclassification.

SJP Sosioedukasi
JURNAL ILMIAH ILMU PENDIDIKAN DAN SOSIAL
ISSN: 2086-6135 E-ISSN: 2541-612x
Volume 15 No. 1. Maret 2026 https://ejournal.unibabwi.ac.id/index.php/sosioedukasi/index

Table 2 Confusion Matrix for Random Forest Classification

Time	Class	Water	Vegetation	Built-Up Land
2000	Water	6	0	0
	Vegetation	1	46	3
	Built-Up Land	0	1	49
2023	Water	17	3	5
	Vegetation	0	49	1
	Built-Up Land	1	1	48

Table source: Analysis Results, 2026

In 2023, the classifier also produced high performance with an OA of 92.00% and a Kappa coefficient of 0.870. Although slightly lower than in 2000, the results still indicate very good agreement. Most classification errors occurred in the water class, which was occasionally confused with vegetation and built-up land, likely due to increased urban complexity and mixed coastal pixels. Vegetation and built-up land maintained high classification accuracy with only minimal errors.

Overall, the comparison suggests that the slight reduction in classification accuracy does not reflect limitations of the Random Forest algorithm itself but rather the changing characteristics of the study area. Rapid urbanization has produced a more heterogeneous landscape with greater spectral variability and more transitional land cover classes, inherently increasing classification difficulty. Nevertheless, the high Overall Accuracy and Kappa values for both years provide strong confidence that the classified land cover maps are sufficiently accurate to support subsequent analyses of land cover change, Land Surface Temperature (LST), and Surface Urban Heat Island (SUHI) dynamics throughout Manado City.

2000

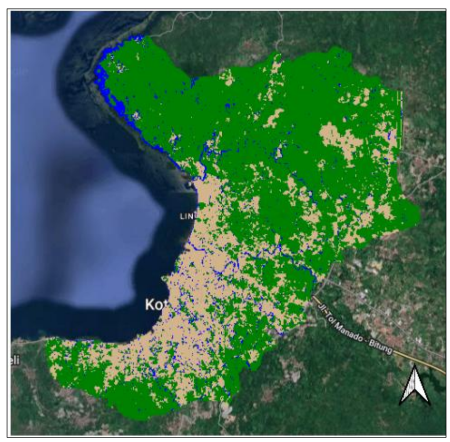

2023

Figure 3 Land Cover Classification Map
Figure source: Analysis Results, 2026

The land cover classification of Manado City in 2000 shows that vegetation was the dominant land cover, covering 75.90% (10,844.523 ha) of the study area (Table 3). Vegetation was widely distributed across the southern, eastern, and northern parts of the city, while built-up land was mainly concentrated in the urban center and coastal areas. Water bodies occupied only a small proportion of the area along the coastline and river systems. This spatial pattern indicates a relatively compact urban form with low landscape fragmentation, which likely contributed to lower surface heating and reduced Surface Urban Heat Island (SUHI) intensity.

SJP Sosioedukasi
JURNAL ILMIAH ILMU PENDIDIKAN DAN SOSIAL
ISSN: 2086-6135 E-ISSN: 2541-612x
Volume 15 No. 1. Maret 2026 https://ejournal.unibabwi.ac.id/index.php/sosioedukasi/index

The 2023 land cover classification reveals substantial urban expansion and vegetation loss. Although vegetation remained the dominant class, its distribution became more fragmented due to the expansion of residential, commercial, and transportation areas. Built-up land expanded outward from the city center, increasing from 23.55% to 27.49%, while water bodies appeared more extensive, partly due to the improved image quality of Landsat 9. Overall, the 2023 map reflects a more urbanized and heterogeneous landscape than in 2000.

Comparison of the two classifications highlights the long-term effects of urbanization between 2000 and 2023. Vegetation decreased by 1,231.50 ha (−8.59%), while built-up land increased by 677.52 ha (+4.72%), resulting in greater landscape fragmentation and reduced green space continuity. These land cover changes are expected to reduce evapotranspiration and increase heat absorption, providing spatial evidence for the observed increase in Land Surface Temperature (LST) and the expansion of the Surface Urban Heat Island (SUHI) in Manado City.

Land Cover Change Results for 2000 and 2023

Land cover in Manado City changed significantly between 2000 and 2023 (Table 3). Vegetation decreased by 1,120.477 ha, from 75.69% to 67.87%, while built-up land increased by 565.327 ha, from 23.55% to 27.49%, indicating the conversion of vegetated areas into urban land. Water bodies also increased by 555.150 ha (0.75%–4.62%), partly due to improved sensor characteristics and classification accuracy. These changes reflect ongoing urban expansion, which reduces natural cooling from vegetation and increases impervious surfaces that absorb heat. As a result, urban growth contributed to the increase in average Land Surface Temperature (LST) from 33.79°C in 2000 to 37.08°C in 2023, supporting the intensification of the Surface Urban Heat Island (SUHI) in Manado City.

Table 3 Comparison of Land Cover Classification Areas in Manado in 2000 and 2023

Class	Year				Change in Area (ha)	
	2000		2023		Luas	%
	Area (ha)	%	Area (ha)	%		
Water	108,051	0.75	663,202	4.62	555,150	+3.87
Vegetation	10.844,523	75.69	9.724,045	67.87	-1.120,477	-7.82
Built-up Land	3.374,629	23.55	3.939,957	27.49	565,327	+3.94

Table source: Analysis Results, 2026

Land Surface Temperature

The analysis results show that the average Land Surface Temperature (LST) in Manado City increased from 2000 to 2023. In 2000, the average LST was recorded at 33.79°C, then rose to 37.08°C in 2023. This increase in surface temperature did not occur uniformly across the entire region but was concentrated in subdistricts with high rates of land-use change. This pattern indicates that changes in LST in Manado City are strongly influenced by land-cover dynamics in each subdistrict, rather than by regional climate factors.

The spatial distribution of Land Surface Temperature (LST) in Manado City in 2000, derived from Landsat 7 ETM+ thermal imagery. The map indicates that lower surface temperatures are predominantly associated with extensive vegetation cover, particularly in the southern and eastern parts of the city where forests and other green spaces remain abundant. These areas exhibit relatively cool thermal conditions due to the cooling effects of evapotranspiration and shading provided by dense vegetation. Conversely, higher surface temperatures are concentrated within the urban core and coastal districts, where built-up land is dominant. The concentration of warmer pixels in these areas reflects the greater heat absorption and storage capacity of impervious materials such as asphalt, concrete, and building roofs. The average LST in 2000 was 33.79°C, indicating that although localized urban warming had already developed within the city center, the overall thermal environment was still moderated by the extensive vegetation that occupied more than three-quarters of the study area. The relatively compact distribution of high-temperature zones suggests that urban heat was primarily confined to established urban districts and had not yet expanded substantially into suburban regions.

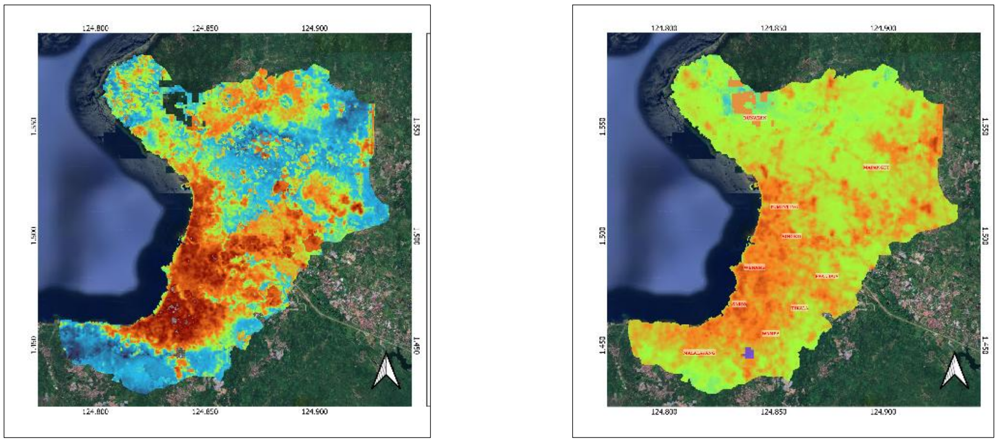

Figure 4 Land Surface Temperature
Figure source: Analysis Results, 2026

The **2023 Land Surface Temperature (LST)** map derived from Landsat 9 OLI/TIRS shows a clear expansion of high-temperature areas across Manado City. The average LST increased from **33.79°C** in **2000** to **37.08°C** in **2023** (+3.29°C), corresponding to the expansion of built-up land and the decline in vegetation. High-temperature zones extended beyond the city center into rapidly developing suburban areas, while lower temperatures remained concentrated in vegetated regions, highlighting the cooling role of urban green spaces.

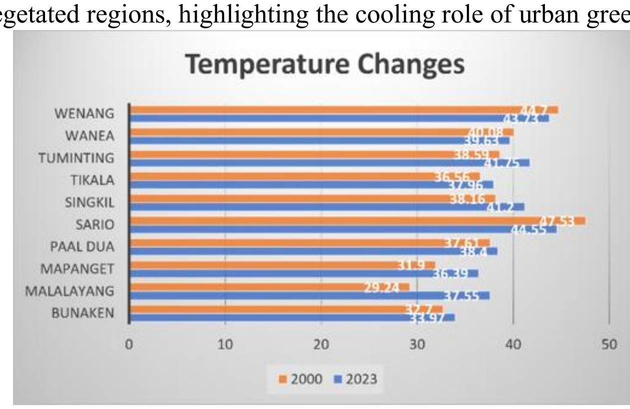

Figure 5 Bar Chart of Temperature Variations Among Subdistricts in Manado City
Figure source: Analysis Results, 2026

Figure 5 shows that almost all subdistricts experienced higher LST in 2023 than in 2000. The greatest increase occurred in Malalayang (+8.31°C), followed by Mapanget (+4.49°C), indicating significant urban development in these areas. Overall, the results demonstrate that surface warming has become more widespread across Manado City, reflecting the effects of continued urban expansion.

Surface Urban Heat Island Results

Figure 6 shows the spatial distribution of Surface Urban Heat Island (SUHI) intensity in Manado City for 2000 and 2023. High SUHI intensity is concentrated in built-up urban areas, while lower intensity occurs in vegetated peripheral regions. Compared with 2000, the 2023 map indicates a wider distribution of high SUHI intensity, reflecting urban expansion and the reduction of vegetation. These results highlight the important role of green spaces in mitigating urban warming.

JURNAL ILMIAH ILMU PENDIDIKAN DAN SOSIAL
ISSN: 2086-6135 E-ISSN: 2541-612x
Volume 15 No. 1. Maret 2026 https://ejournal.unibabwi.ac.id/index.php/sosioedukasi/index

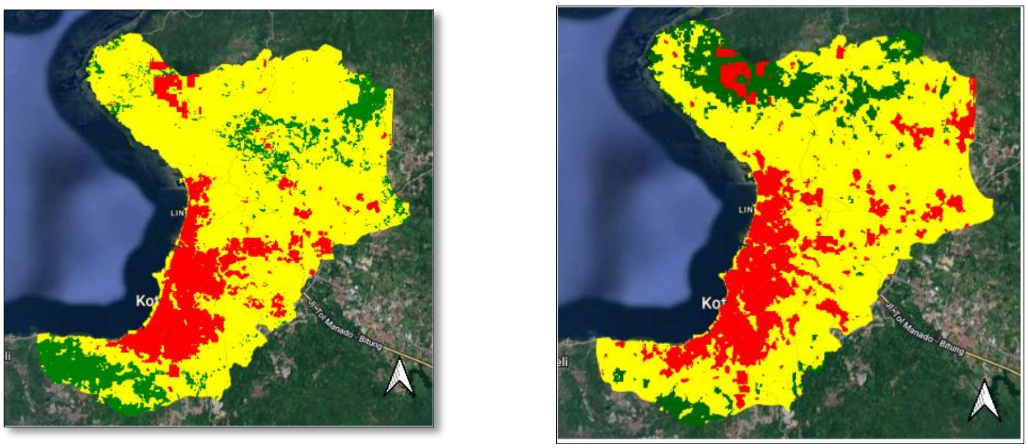

Figure 6 Map of the Surface Urban Heat Island in Manado
Figure source: Analysis Results, 2026

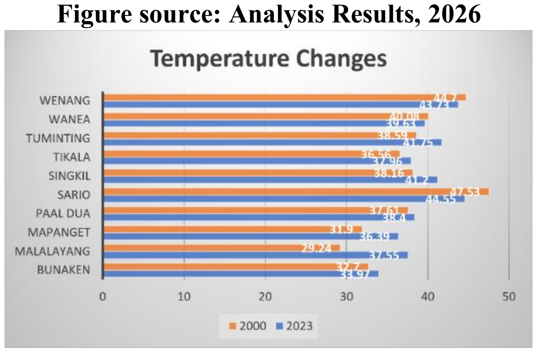

Figure 7 Bar Chart of Temperature Variations Among Subdistricts in Manado City
Figure source: Analysis Results, 2026

Figure 7 compares SUHI intensity across Manado City's subdistricts in 2000 and 2023. Most subdistricts experienced increased SUHI intensity, with larger increases occurring in areas undergoing rapid urban development. In contrast, subdistricts with greater vegetation cover showed relatively lower SUHI intensity. These findings indicate that land cover change, particularly the expansion of built-up land at the expense of vegetation, is the primary driver of SUHI intensification in Manado City.

Discussion

The accuracy assessment indicates that the 2000 land cover classification achieved slightly higher accuracy than the 2023 classification, likely due to increasing urban heterogeneity, which makes land cover classes more difficult to distinguish. This finding is consistent with (Zhao et al., 2025) who state that the heterogeneity of urban areas can reduce the accuracy of satellite image classification.Urban expansion in Manado City was accompanied by vegetation loss, an increase in built-up land, and a rise in average Land Surface Temperature (LST). The reduction of vegetation decreased natural cooling through evapotranspiration, while the expansion of impervious surfaces increased heat absorption and storage, contributing to the intensification and wider spatial distribution of the Surface Urban Heat Island (SUHI). The lower SUHI standard deviation in 2023 suggests that urban warming has become more widespread across the city.

Spatially, Malalayang and Mapanget experienced the largest increases in LST, whereas Sario and Wenang consistently recorded the highest SUHI intensity, reflecting the influence of dense built-up areas. In contrast, Malalayang exhibited lower SUHI intensity despite a large increase in LST, likely due to the moderating effects of vegetation and its coastal location. Mapanget also recorded the highest population growth, indicating that suburban expansion has contributed to increasing surface temperatures. However, the consistently high SUHI values in Sario and Wenang despite relatively low population growth suggest that land cover and built-up density have a greater influence on urban thermal conditions than population growth alone.

The findings of this study align with those of Wardhana (2021), which indicate that an increase in built-up areas contributes to a rise in urban surface temperatures (Wardhana et al., 2021). Additionally, vegetation plays a crucial role in lowering temperatures through evapotranspiration and shading effects (Puri, 2025). Similar results were found in a study by Dani (2026), which stated that a decrease in vegetation and an increase in the density of built-up areas can raise urban temperatures and degrade environmental quality (Dani et al., 2026). Thus, changes in land cover are a major factor that influences the development of the Urban Heat Island phenomenon in Manado City.

CONCLUSION

This study shows that significant changes in land cover have occurred in the city of Manado during the 2000 and 2023 period, marked by an 7,82% decrease in vegetation and a 3,94% increase in built-up land. These changes were accompanied by an average increase in Land Surface Temperature (LST) of 3.29°C, as well as an expansion and more even distribution of urban heat, as indicated by a decrease in the standard deviation of the Surface Urban Heat Island (SUHI) values. The research results also indicate that SUHI dynamics are not only influenced by changes in land cover but are also related to population growth patterns across subdistricts, including both rapidly developing areas and older urban areas that are already development-saturated. The use of Google Earth Engine and the Random Forest algorithm proved effective in supporting this integrated analysis

REFERENCES

Badan Pusat Statistika. (2023). *Kota Manado Dalam Angka 2023*. BPS Kota Manado.

Dani, L., Hakim, S. P., Fitria, M., Lestari, S. M., Supendi, A., Fauzi, M. S. E., Raudya Setya Wismoko Purti, M. P., Pd, M., Handayani, N., Par, M., Amiruddin, I., Fisu, A., Fitriyanti, M. A., Azmi, U., Ars, S., Ars, M., Zani, N. M., Azizah, M. P. W. K., & Abdi, P. (2026). *Tata Ruang dan Tata Guna Lahan* (Kafariska, Ed.). CV.Brizqha Media Qit BriMeta Publisher. www.brimetapublisher.com

Darmawan, S., Nurulhakim, N. N., & Hernawati, R. (2024). Kecerdasan Buatan berbasis Geospasial (GeoAI) menggunakan Google Earth Engine untuk Monitoring Fenomena Urban Heat Island di Indonesia. *ELKOMIKA: Jurnal Teknik Energi Elektrik, Teknik Telekomunikasi, & Teknik Elektronika*, *12*(2), 303. https://doi.org/10.26760/elkomika.v12i2.303

Elwantyo, B., Dewantoro, B., Natani, P. A., & Islamiah, Z. (2020). *Analisis Surface Urban Heat Island menggunakan Teknik Penginderaan Jauh Berbasis Cloud Computing pada Google Earth Engine di Kota Samarinda*.

Fawzi, N. I. (2017). Mengukur Urban Heat Island Menggunakan Penginderaan Jauh Kasus Di Kota Yogyakarta. *MAJALAH ILMIAH GLOBE*, *19*(2), 195. https://doi.org/10.24895/mig.2017.19-2.603

Kartika, S., Sanjaya, H., & Muhardi. (2024). Pemantauan Fenomena Urban Heat Island di Kota Pontianak, Kalimantan Barat, Menggunakan Google Earth Engine. *POSITRON*, *14*(2), 108–117. https://doi.org/10.26418/positron.v14i2.71475

Lu, Y., He, T., Xu, X., & Qiao, Z. (2021). Investigation the Robustness of Standard Classification Methods for Defining Urban Heat Islands. *IEEE Journal of Selected Topics in Applied Earth Observations and Remote Sensing*, *14*, 11386–11394. https://doi.org/10.1109/JSTARS.2021.3124558

Natun, N. C. I., & Sumarlin, S. (2025). Analisis Perbandingan Klasifikasi Supervised dan Unsupervised Citra Satelit Landsat Untuk Pemetaan Penutupan Lahan di Kabupaten Kupang. *Jurnal Manajamen Informatika Jayakarta*, *5*(2), 142. https://doi.org/10.52362/jmijayakarta.v5i2.1812

Puri, P. (2025). Advanced Spatio-Temporal Analysis of Surface Urban Heat Island Intensity in the Mumbai Metropolitan Region Using Surface Imperviousness, Land Use- Land Cover, and Local Climate Zones Via Google Earth Engine and Deep Learning (2003–2023). *Journal of Landscape Ecology (Czech Republic)*, 79–108. https://doi.org/10.2478/jlecol-2026-0014

Rahman, D. R., Sandrawati, A., & Siswanto, S. Y. (2022). Identifikasi Penggunaan Lahan dan Analisis Kesesuaian Pola Ruang menggunakan Citra Landsat 8 OLI Tahun 2020 (Studi Kasus: Sub-DAS Cikeruh, Citarik, dan Cirasea. *Jurnal Ilmu Tanah Dan Lingkungan*, *24*(2), 79–86. https://doi.org/10.29244/jitl.24.2.79-86

Safitri, R., Vonnisa, M., & Marzuki, M. (2022). Analisis Dampak Perubahan Tutupan Lahan di Kalimantan Terhadap Temperatur Permukaan. *Jurnal Fisika Unand*, *11*(2), 173–179. https://doi.org/10.25077/jfu.11.2.173-179.2022

Stewart, I. D., & Mills, G. (2021). *The Urban Heat Island*. Elsevier.

USGS. (2020). *Landsat Collection 2 Surface Temperature*. USGS. https://www.usgs.gov/landsat-missions/landsat-collection-2-surface-temperature

Wardhana, F., Jaya, G., Saleh, F., & Karim, J. (2021). Pemetaan Fenomena Urban Heat Island Di Kota Kendari Dengan Menggunakan Citra Resolusi Menengah. *JAGAT : Jurnal Geografi Aplikasi Dan Teknologi*.

Zhao, L., Fan, X., & Hong, T. (2025). Urban Heat Island Effect: Remote Sensing Monitoring and Assessment—Methods, Applications, and Future Directions. *Atmosphere*, *16*(7). https://doi.org/10.3390/atmos16070791